Molecular Crystals and Liquid Crystals

Publication details, including instructions for authors and subscription information:
http://www.tandfonline.com/loi/gmcl20

Simultaneous X-ray and Visible Light Diffraction for the Investigation of Surface Relief and Density Grating Formation in Azobenzene Containing Polymer Films

Oliver Henneberg [a], Ullrich Pietsch [a], Tobias Panzner [a], Thomas Geue [b] & Ken Finkelnstein [c]

[a] Institute of Physics, University of Potsdam, Potsdam, Germany

[b] Paul Scherrer Institute, Villigen PSI, Switzerland

[c] CHESS, Cornell University, Wilson Laboratory, Ithaca, New York, USA

Version of record first published: 16 Aug 2006

To cite this article: Oliver Henneberg, Ullrich Pietsch, Tobias Panzner, Thomas Geue & Ken Finkelnstein (2006): Simultaneous X-ray and Visible Light Diffraction for the Investigation of Surface Relief and Density Grating Formation in Azobenzene Containing Polymer Films, Molecular Crystals and Liquid Crystals, 446:1, 111-121

To link to this article: http://dx.doi.org/10.1080/15421400500383345

Mol. Cryst. Liq. Cryst., Vol. 446, pp. 111–121, 2006

ISSN: 1542-1406 print/1563-5287 online
DOI: 10.1080/15421400500383345

Taylor & Francis
Taylor & Francis Group

Simultaneous X-ray and Visible Light Diffraction for the Investigation of Surface Relief and Density Grating Formation in Azobenzene Containing Polymer Films

Oliver Henneberg
Ullrich Pietsch
Tobias Panzner
Institute of Physics, University of Potsdam, Potsdam, Germany

Thomas Geue
Paul Scherrer Institute, Villigen PSI, Switzerland

Ken Finkelnstein
CHESS, Cornell University, Wilson Laboratory, Ithaca, New York, USA

The development of surface relief and density patterns in azobenzene polymer films was studied by diffraction at two different wavelengths. We used x-ray diffraction of synchrotron radiation at 0.124 nm in combination with visible light diffraction at a wavelength of 633 nm. In contrast to visible light scattering x-ray diffraction allows the separation of a surface relief and a density grating contribution due to the different functional dependence of the scattering power. Additionally, the x-ray probe is most sensitive for the onset of the surface grating formation.

Keywords: azobenzene polymer; surface relief grating; x-ray scattering

INTRODUCTION

It is known since 1995 that a surface relief pattern can be inscribed on a polymer film containing azobenzene moieties [1,2]. Suitable light

The support from DFG Pi 217/3 is kindly acknowledged. This work is based upon research conducted at the Cornell High Energy Synchrotron Source (CHESS) which is supported by the National Science Foundation and the National Institutes of Health/National Institute of General Medical Science under award DMR 9713424.

Address correspondence to Oliver Henneberg, Institute of Physics, University of Potsdam, D-14415 Potsdam, Germany. E-mail: ohenneberg@gadir.physik.uni-potsdam.de

initiates a cycling of cis-trans and trans-cis isomerisations of the azobenzene moieties and subsequent co-operative interactions with the polymer main chain and the side groups. Within the interference pattern the polarization and/or the intensity of the incident light changes periodically and with it the strength of interaction with the azobenzene units. This results in a surface relief grating of nearly sinusoidal shape (Fig. 1). The surface relief grating formation takes place at room temperature, i.e., far below the glass transition temperature of the polymer material. Depending on laser power the profile depth of the surface relief grating may reach 100 nm after few minutes of exposure. A number of mechanism has been proposed to explain the surface relief grating formation [3–6] but they fail in the overall interpretation of the formation dynamics.

For the polymer pDR1M we have shown that a lateral density grating is formed in addition to the surface relief grating during light inscription [7]. Heating the sample up to T_g the surface relief grating disappears but a certain amount of the density grating may remain. This property might be the origin of the phenomenon appearing at pDR1M only, that a new grating can be formed annealing the sample at a temperature much higher then T_g [8]. This grating has the same period as the initial surface relief grating and is formed under illumination of read light only. The nature of this high-temperature density

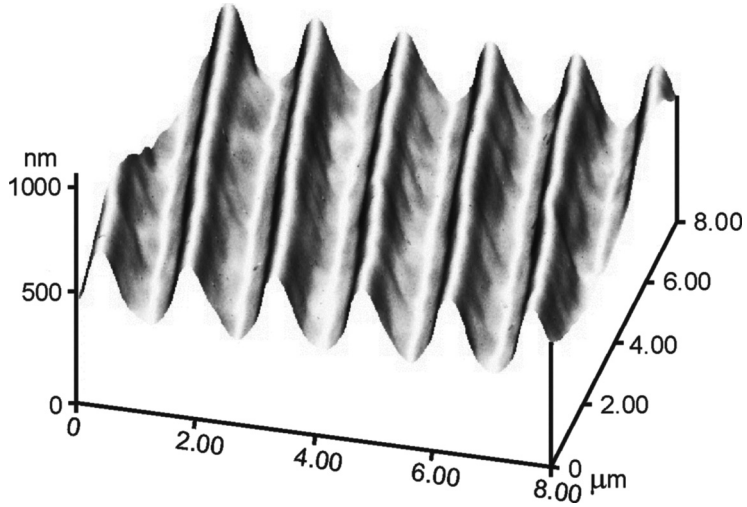

FIGURE 1 AFM image of a polymer surface relief grating with sinusoidal height profile.

grating is not fully understood yet but it is stable against any further temperature treatment [9].

X-ray reflectivity using synchrotron radiation can be used to evaluate the dynamics of surface relief grating and density grating formation [10]. Based on a scattering approach being valid for both x-ray and visible light scattering one is able to distinguish between the contribution of the density grating and the surface relief grating due to their different functional dependencies on grating height and the density difference [11]. It became obvious that x-ray scattering is most sensitive for the onset of grating formation due to the much larger momentum transfer compared to visible light.

In this paper we present a combined x-ray and visible light scattering experiment where we have observed the grating formation *in-situ*. It revealed that both density grating and surface relief grating are formed with a different time dependence.

EXPERIMENTAL

The azobenzene containing polymer of pDR1M (poly{(4-nitrophenyl) [4-[[2-(methacryloyloxy)ethyl]ethylamino]phenyl]diazene}) (Fig. 2) with a glass transition temperature of $T_g = 130^{\circ}C$ was dissolved in THF and spun onto a float glass substrate. The flat polymer films with thickness of about 200 nm were dried for about 10 hours at 60°C to remove remaining solvent. The surface relief gratings were prepared using an interference pattern of two coherent laser beams at $\lambda_{writing} = 488\,nm$ leading to a periodic spatial variation of intensity and/or polarization direction. In order to illuminate a large sample area the beam of the Ar^+ laser with diameter of 0.8 mm was expanded with a reversed Kepler system to a diameter of 30 mm. From Gaussian intensity distribution the central part was cut by a circular diaphragm. Only this part of the beam was used for inscribing the surface relief grating with a maximum power density of $P = 20\,mW/cm^2$. The linear polarization of the laser was changed into circular polarization using a quarter wave plate.

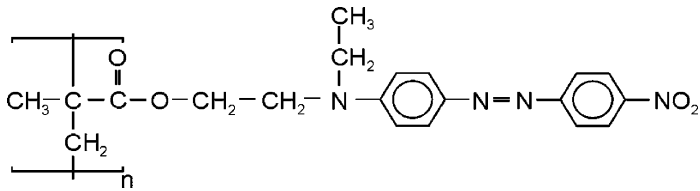

FIGURE 2 Structure formula of pDR1M in trans conformation.

In order to investigate the dynamics of grating formation by *in-situ* x-ray scattering the writing setup was installed at the C-line of Cornell High Energy Synchrotron Source (CHESS) on a heavy and vibration damped Huber 4-circle diffractometer. In order to minimize vibrations the circular beam was split into two partial beams using a prism right in front of the sample (Fig. 3). One semi-circle hits the sample in normal incidence. After reflection at a mirror the second semicircle falls with an angle γ onto the same spot of the sample. This results in an interference pattern on the sample surface with a lateral spacing of $D = \lambda_{\text{writing}}/\sin\gamma$. Using $\gamma = 24^\circ$ we achieved a period of $D = 1200\,\text{nm}$. A red diode laser with wavelength $\lambda_{\text{vis}} = 633\,\text{nm}$ was diffracted by the created grating and the first order diffraction was detected with a photo diode and recorded with a lock-in amplifier.

A Si 111 crystal was used to select the $\lambda_{\text{x-ray}} = 0.124\,\text{nm}$ from a bending magnet radiation. The x-ray beam size could be adjusted with a slit system to a spot of 1 mm width and 0.07 mm in height. The x-ray footprint on the sample is $1 \times 6\,\text{mm}^2$ at an incident angle of $\alpha_i = 0.7^\circ$.

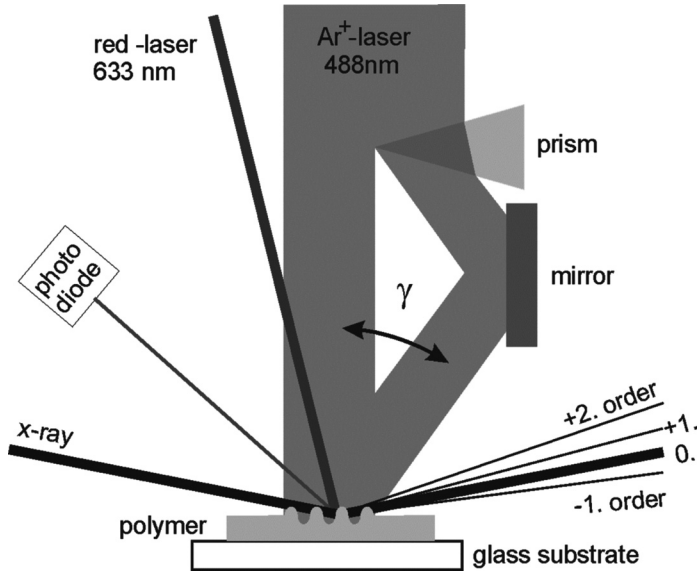

FIGURE 3 Set-up used for *in-situ* inspection of grating formation using laser interference at $\lambda_{\text{writing}} = 488\,\text{nm}$ and combined x-ray and laser light scattering. The diffracted laser light of $\lambda_{\text{vis}} = 633\,\text{nm}$ is detected in reflection geometry by a photodiode. The diffracted synchrotron radiation $\lambda_{\text{x-ray}} = 0.124\,\text{nm}$ strikes the sample at a shallow angle and the scattered beams are detected with a CCD (not shown).

During laser writing the x-rays were diffracted at the forming grating giving rise to several grating peaks similar to conventional optics. Several of these grating peaks could be recorded simultaneously with a CCD camera. The CCD camera (Quantum) had 1024×1024 pixel and a 16 bit dynamic range. Reducing the read-out region to 60×1024 pixel the read-out time could be reduced to 7 seconds. Illumination time was one second each. At the same time the photo diode recorded the first order diffraction from red probe laser quasi continuous. This unique setup allows simultaneous time-resolved investigation of surface relief grating and density grating formation with x-ray and laser light [12].

SCATTERING THEORY

The physical origin of the diffraction from electromagnetic waves on periodic structures depends on the scattered wavelength. For visible light it is the refractive index n which has to be taken into account while for x-rays one has to consider the electron density ρ. In addition, x-ray diffraction is performed mostly at shallow angles with respect to the sample surface where one can approximate $\sin \alpha \approx \alpha$ in most cases. The Bragg equation for scattering of plane waves of wavelength λ at a periodic grating D can be expressed by

$$m\lambda = D(\cos \alpha_f - \cos \alpha_i) \tag{1}$$

where α_i and α_f are the incident and exit angle with respect to the surface and m is the diffraction order [13]. Using visible light ($\lambda_{vis} = 633\,nm$) and a grating period $D = 1200\,nm$ the number of visible grating peaks in the whole half-space is $m = 3$ ($m\lambda \leq 2D$). For x-rays with a wavelength of $\lambda_{x\text{-}ray} = 0.124\,nm$ the number of possible diffraction orders m becomes very large. However, the quantum of measurable peaks is restricted to an angular range close to the specular reflected beam ($\alpha_f = \alpha_i$) because the intensity of the I_m decreases with increasing m. Scattering is typically expressed in reciprocal space. The real space coordinates can be transformed into reciprocal space ones by

$$q_x = k(\cos \alpha_f - \cos \alpha_i) \tag{2a}$$

$$q_z = k(\sin \alpha_f + \sin \alpha_i) \tag{2b}$$

with the wave vector $k = 2\pi/\lambda$. In reciprocal space the distance between two grating peaks is equidistant $\Delta q_x = q_D = 2\pi/D$ and the position of the mth order grating peak is at $q_x = m2\pi/D$.

If we investigate the development of a surface grating the grating height h depends on the position x and the time t. Both parts can be separated

$$h(x,t) = h_{\max}(t)\cos(\Delta q_x x). \tag{3}$$

where $h_{\max}$ is usually simply called "grating height".

At the same time a density grating is forming, which can be expressed by a Fourier series of the refraction index n

$$n(x) = n(1 + B_1\cos(\Delta q_x x) + B_2\cos(2\,\Delta q_x x) + \cdots) \tag{4}$$

where B_1 and B_2 are the 1st and 2nd order Fourier coefficients. In x-ray scattering $n(x)$ is replaced by the electron density $\rho(x)$.

Both gratings contribute to the scattering amplitude A but with different functional dependencies. At the position of mth grating maximum the x-ray scattering amplitudes $A_{\text{x-ray}}$ is

$$A_{\text{x-ray}}(q_x = mq_D) = J_m(q_z h_{\max}) - \exp(iq_z d)\frac{B_m}{2} \tag{5}$$

Here the grating height is included in the argument of the mth order Bessel function J_m, whereas the density variation is expressed by the mth Fourier coefficient B_m. Therefore the contribution of the surface grating to the scattering amplitude oscillates although the grating height $h_{\max}$ is continuously increasing! On the other side the contribution of the density grating is increasing with increasing density B_m. The measured intensity I is calculated with the complex conjugated $A(q)^*$ of the scattering amplitude $A(q)$, $I = AA^{*\surd}$.

Straight after turning the writing laser on the 1st order x-ray grating peak intensity $I_{\text{x-ray}}$ increases due to the growth of grating height up to $h_{\max} \approx 2\,\text{nm}$ and decreases afterwards toward zero if there is no additional contribution of a density grating ($B_m = 0$). In case of the appearance of a density grating ($B_m > 0$) the intensity saturates at a certain value which depends on the film thickness d. The different functional dependence of the x-ray scattering amplitude from grating height and density difference allows separation of both the surface relief grating and the density grating.

These functional dependences differ for visible light scattering. Here the scattering amplitude is given by

$$A^{VIS}(q_x^{VIS} = mq_D) = J_m(q_z^{VIS} h_{\max}) - \exp(iq_z^{VIS} d)J_m(q_z^{VIS} P_m d) \tag{6}$$

where $q_{\text{x}}^{\text{VIS}}$ and $q_{\text{z}}^{\text{VIS}}$ are calculated according to Eqs. (2a), (2b) and wavelength $\lambda_{\text{VIS}} = 633\,\text{nm}$. The contribution of the density grating is expressed by a Fourier series of the optical refraction index $n(x)$ with

the coefficients P_m. In contrast to x-ray scattering both gratings are expressed by Bessel functions J [11].

The main difference in x-ray and visible light scattering is the amount of momentum transfer q_z. Due to the longer wavelength it is 100 times smaller for visible light scattering than for x-rays ($100\ q_z^{\mathrm{VIS}} \approx q_z^{\text{x-ray}}$). Therefore the first (main) maximum and further oscillations of visible light intensity are expected for grating heights $h_{\max} \gg 100\,\mathrm{nm}$.

RESULTS

The grating formation was studied under permanent holographic exposure by the writing Ar^+ laser. The x-ray diffraction is shown for 8 snapshots of CCD images of a time series (Fig. 4). For virgin samples and no laser power there are no peaks except the specular reflected one ($\alpha_f = \alpha_i$). This situation is shown for x-rays in Figure 4 for $t = 0\,\mathrm{s}$. Immediately after the laser is turned on the 1st order x-ray peak appear in plus ($\alpha_f > \alpha_i$) and minus ($\alpha_f < \alpha_i$) direction (Fig. 4, image at $t = 60\mathrm{s}$). Further grating orders appear later in time (see further frames in Fig. 4). Finally we could observe up to 16 grating peaks in one CCD image (see $t = 600\,\mathrm{s}$).

In order to extract the time development of individual grating peaks the individual peaks of each image were integrated and subtracted from background. For the 1st, 2nd and 3rd grating peak the time

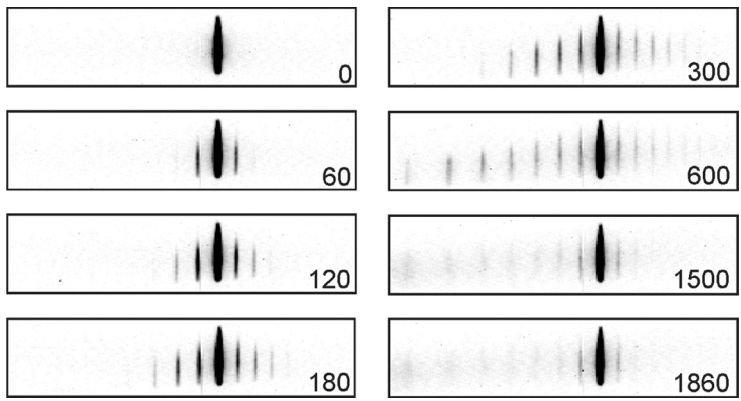

FIGURE 4 The time series of CCD images shows the development of several grating peaks beside the specular maximum (black spot in center). The numbers indicate the time after switching on the writing laser at $\lambda_{\mathrm{writing}} = 488\,\mathrm{nm}$.

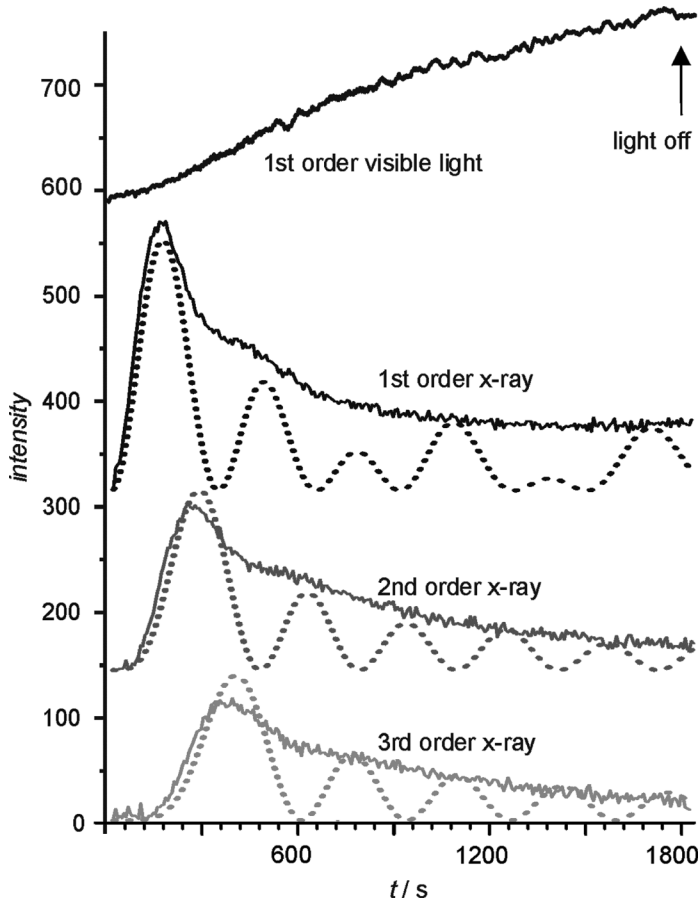

FIGURE 5 Development of the visible light (upper line) and the 1st to 3rd x-ray (lower lines) diffraction intensities (full lines). The dotted lines were calculated, details see text.

development is shown in the lower part of Figure 5. Additionally the diffraction signal of the visible light diffraction is plotted in the top graph of Figure 5. The 1st order x-ray diffraction peak reaches an intensity maximum after 100 seconds (Fig. 5, second graph). Afterwards the intensity drops down, oscillates slightly and finally keeps constant. The higher order peaks show similar behavior, but less pronounced (Fig. 5, third and fourth graph). At the same time the intensity of the visible laser light diffraction does increase monotonic until the laser is turned of at time $t = 1800$ s.

In Figure 5 it can clearly be seen that the time where the intensity maximum of $m$the grating peak appears increases with the order m. This is caused by the fact that the main maximum of Bessel function J_m appears for higher $h_{\max}$ increasing order m. Considering this functional dependence and using the time of reaching the maximum intensity of J_m one can calculate $h_{\max}(t)$ and subsequently the growth velocity v. The growth velocity varies as a function of the polarization state of the inscribing laser beam and reaches its maximum if the interference pattern is built by two circular polarized laser beams. Using a laser power of $p = 20\,\mathrm{mW/cm^2}$ the grating height growth linear in time and the growth velocity is $v = 0.018\,\mathrm{nm/s}$.

In order to simulate the time development of single grating peak intensity one has to consider the development of a surface relief grating and a density grating. First, one finds that the intensity decreases monotonic after reaching the main maximum and does not oscillate as suggested by the Bessel function. This leveling of oscillations is caused by the fact that the grating height is not uniform within the illuminated sample area. It decreases nearly uniform from one side to the other. Additionally one has to consider that the spatial distribution of Ar^+-laser intensity is not uniform but shows Gaussian distribution. Therefore the growth rate is higher in the center of the sample than at its borders. In reality the measured intensity is the envelope of many slightly different Bessel functions.

Second, significant saturation above zero intensity could observed at 1st order peak, only. The intensity of the other grating peaks vanishes at longer illumination time. The remaining intensity of the last two graph of Figure 4 ($t = 1500$ and $1860\,\mathrm{s}$) are caused by diffuse bulk scattering. Thus, the density grating can be described by its first Fourier component B_1, (See Eq. (5)) representing a pure sinusoidal density variation.

Considering the height distribution of the sample mentioned above the time development of grating intensity can be simulated by means of Eq. (5) using $h_{\max}(t)$ and $B_1(t)$ as parameters. The result of this simulation is shown as dotted lines in Figure 5. Here the nonuniformity mentioned above was approximated by an average grating height $\langle h_{\max} \rangle$. Considering the linear time development of $\langle h_{\max} \rangle$ one finds a nonlinear time development of $B_1(t)$, i.e., the density grating develops in the first 10 minutes and afterwards it stays constant (see Fig. 6).

At the same time the visible light scattering can be simulated using Eq. (6). The maximum height of the formed grating was about $h_{\max} \approx 20\,\mathrm{nm}$ which has been verified by AFM measurement. The Bessel function of the visible light scattering would reach its first

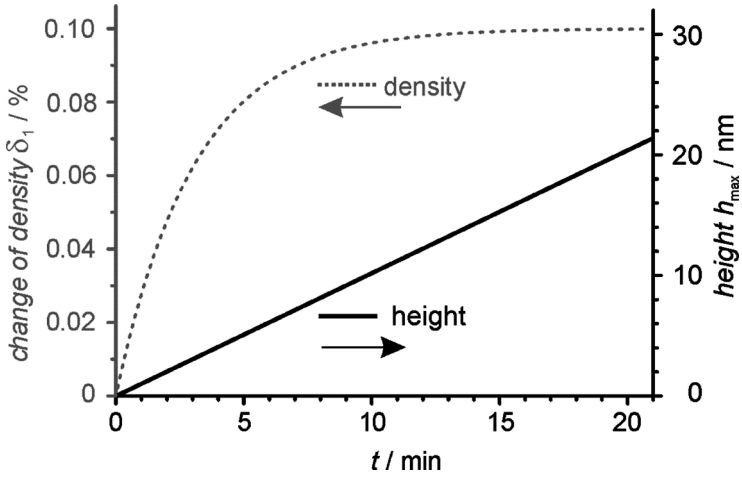

FIGURE 6 Time development of grating height (right axis) and density difference (left axis) evaluated from the time development of x-ray scattering intensities shown in Figure 5.

maximum at a height of $h_{\max} \approx 200\,\text{nm}$, which explains the almost linear rise of visible light scattering intensity in the investigated time interval.

CONCLUSION

It has been shown that x-ray diffraction has a much higher sensitivity for small grating heights in comparison with laser light scattering. For grating heights below 10 nm x-ray scattering is much better suited than diffraction by visible light. For visible light diffraction both contributions are described by Bessel function. Separation of both contributions requires measurement with two different wave lengths (paper Rochon + Pietsch). Combined x-ray and visible light scattering allows inspection of grating formation from early beginning up to the maximum grating height. It was shown that even in the initial state of grating formation the density grating contributes with significant amount to the total scattering signal.

Light induced surface relief grating formation has been observed at various polymer materials. In most cases it has been probed by atomic force microscopy and visible light scattering. The density grating is part was not considered so far but one can assume that density grating formation is an inherent part of each of these polymer gratings. This requires further investigation.

REFERENCES

[1] Rochon, P., Batalla, E., & Natansohn, A. L. (1995). *Appl. Phys. Lett.*, *66*, 136.
[2] Kim, D. Y., Tripathy, S. K., Li, L., & Kumar, J. (1995). *Appl. Phys. Lett.*, *66*, 1166.
[3] Barrett, C. J., Natansohn, A. L., & Rochon, P. (1996). *J. Phys. Chem.*, *100*, 8836.
[4] Kumar, J., Li, L., Jiang, X. L., Kim, D. Y., Lee, T. S., & Tripathy, S. K. (1998). *Appl. Phys. Lett.*, *72*, 2096.
[5] Bian, S., Williams, J. M., Kim, D. Y., Li, L., Balasubramanian, S., Kumar, J., & Tripathy, S. K. (1999). *J. Appl. Phys.*, *86*, 4498.
[6] Viswanathan, N. K., Balasubramanian, S., Li, L., Tripathy, S. K., & Kumar, J. (1999). *Jap. J. Appl. Phys.*, *38*, 5928.
[7] Pietsch, U., Rochon, P., & Natansohn, A. L. (2000). *Adv. Mat.*, *12*, 1129.
[8] Geue, T. O., Henneberg, O., Grenzer, J., Pietsch, U., Natansohn, A. L., Rochon, P., & Finkelstein, K. (2002). *Colloids & Surfaces*, *198–200*, 31.
[9] Pietsch, U. & Rochon, P. (2003). *J. Appl. Phys.*, *94*, 963.
[10] Geue, T. M., Saphiannikova, M. G., Henneberg, O., Pietsch, U., Rochon, P. L., & Natansohn, A. L. (2003). *J. Appl. Phys.*, *93*, 3161.
[11] Pietsch, U. (2002). *Phys. Rev.*, *B66*, 155430.
[12] Henneberg, O., Geue, T. H., & Pietsch, U. (2003). *J. Phys. D: Appl. Phys.*, *36*, A241.
[13] Gaylord, T. K. & Moharam, M. G. (1985). *Proc. IEEE*, *73*, 894.